Polymer Chemistry

ROYAL SOCIETY OF CHEMISTRY

PAPER

View Article Online
View Journal | View Issue

Cite this: *Polym. Chem.*, 2023, **14**, 2724

Solvent-free, photoinduced block copolymer synthesis from polymerizable eutectics by simultaneous PET-RAFT and ring-opening polymerization in air†

Yeasmin Nahar,‡ Melissa K. Stanfield, ‡ Alex C. Bissember and Stuart C. Thickett *

Received 20th March 2023,
Accepted 10th May 2023

DOI: 10.1039/d3py00294b

rsc.li/polymers

We report the preparation of poly(*N*-isopropylacrylamide)-*block*-poly(ε-caprolactone) (pNIPAM-*b*-pCL) block copolymers *via* the simultaneous RAFT polymerization and anionic ring-opening polymerization (ROP) of NIPAM and CL respectively, in the absence of traditional solvents. This was achieved through the formation of a deep eutectic solvent system based on mixtures of NIPAM and CL in various mole ratios, which resulted in a viscous liquid at room temperature. 1D and 2D NMR spectroscopy supported the strong association between NIPAM and CL within the eutectic structure and low-self diffusion coefficients of the monomers within the medium. Through the use of a modified RAFT agent with a terminal hydroxyl group on the R group to facilitate ROP, block copolymers were synthesized *via* simultaneous photoinduced-electron/energy transfer RAFT (PET-RAFT) and ROP in air using a ruthenium photocatalyst and tin(II) 2-ethylhexanoate as initiator for the respective polymerizations. Low dispersity copolymers were prepared that exhibited living behaviour; the block copolymers displayed thermoresponsive self-assembly behaviour in water due to the presence of the NIPAM block. The use of the polymerizable eutectic gave much higher reaction rates in comparison to the equivalent reactions conducted in typical organic solvents, highlighting the benefit of this synthetic approach.

Introduction

Reversible-deactivation radical polymerization (RDRP) techniques have transformed polymer science due to their ability to precisely control the molar mass, dispersity, and architectures of polymers.[1] The most commonly employed RDRP techniques include atom-transfer radical polymerization (ATRP),[2] nitroxide-mediated polymerization (NMP),[3] and reversible addition–fragmentation chain-transfer polymerization (RAFT).[4,5] More recently, these established approaches have been augmented by photocatalysis, which can facilitate these processes at ambient temperature under irradiation with visible light,[6–8] as well as in the presence of air,[9,10] removing the need for tedious degassing procedures.

The versatility of degenerative chain transfer agents (CTAs) to control various monomer classes makes RAFT polymerization arguably the most versatile of the different RDRP techniques. Notably, the CTA not only controls the polymerization through the rapid RAFT equilibrium, but also provides an alternative mode for initiating polymerization in the presence of visible light as many CTAs contain appropriate chromophores.[11] Photoinduced RAFT polymerization methods have already been integrated into emerging synthetic techniques such as additive manufacturing and flow chemistry methods.[12,13]

The variety of block copolymers that can be accessed synthetically has greatly expanded by using a dual-functional CTA/initiator, enabling both RDRP and ring opening polymerization (ROP) to occur from the same molecule. This results in block copolymers with blocks derived from distinct reaction mechanisms.[14–17] Such block copolymers are usually prepared in a stepwise manner, typically through using a CTA bearing an appropriate functionality to also initiate ROP; the RAFT agent is used to first control the RDRP of a vinyl monomer, followed by ROP of a relevant lactone (or *vice versa*)[18–23] in the presence of an appropriate catalyst.[24] Simultaneous RDRP/ROP is also possible; "click" chemistry methods to efficiently link homopolymers to form block copolymers with such a composition have also been reported.[25] The development of photoinduced electron/energy transfer RAFT (PET-RAFT) polymerization,[9,26–29] has enabled controlled polymerization

School of Natural Sciences – Chemistry, University of Tasmania, Hobart, Tasmania, 7001, Australia. E-mail: stuart.thickett@utas.edu.au

†Electronic supplementary information (ESI) available. See DOI: https://doi.org/10.1039/d3py00294b

‡These authors contributed equally to this work.

to proceed under mild conditions. In this manifold, the energy provided by visible light obviates the need for thermal initiation. These conditions are compatible with other modes of polymerization, such as orthogonal block copolymerization. For example, the Boyer group demonstrated this through the preparation of poly(ε-caprolactone)-*b*-poly(methyl acrylate) (PCL-*b*-PMA) block copolymers by either sequential or simultaneous ROP and PET-RAFT polymerization.[26]

The majority of polymer syntheses *via* both RDRP and ROP techniques are typically performed in common organic solvents (*e.g.*, DMSO, THF, DMF and toluene). Block copolymer synthesis, with the exception of polymerization-induced self-assembly methods,[30] also requires judicious choice of solvent to ensure the solubility of both blocks. As an alternative to organic solvents, deep eutectic solvents (DESs)[31–33] have enjoyed significant attention in recent times as alternatives to organic solvents and ionic liquids in chemical synthesis,[34,35] including in polymer science.[36] These DESs are remarkably simple to prepare, often *via* the physical mixing of two or more components to form a viscous liquid that possesses a melting point that is significantly lower than any of the individual components.[36,37] DESs can be prepared from non-toxic and naturally abundant starting materials.[38] These systems typically display low volatility, are non-flammable, may be recycled/recovered and possess high thermal and chemical stability. The most common class of DESs are prepared by mixing a hydrogen bond donor (*e.g.*, a carboxylic acid, alcohol or amide) with a hydrogen bond acceptor (*e.g.*, a quaternary ammonium halide salt) in an appropriate stoichiometric ratio.

DES systems have been extensively studied within the context of free-radical polymerization for the preparation of cross-linked gels *via* frontal polymerization,[39–42] polymer monoliths,[43–46] and photo-curing systems.[47–50] These are usually termed 'polymerizable eutectics' (PEs),[51] whereby one or more components of the DES is a polymerizable compound and hydrogen bond donor, such as (meth)acrylic acid, acrylamide and *N*-isopropylacrylamide (NIPAM). There are relatively few reports of RDRP in DES systems and, importantly, these are not PEs – the DES systems used are a direct replacement for a conventional solvent. Examples include the supplemental activator and reducing agent (SARA)[52] and ARGET[53] ATRP of a variety of acrylates and methacrylates in reline (a DES consisting of a 2 : 1 mixture of urea and choline chloride), as well as the ATRP of MMA catalyzed by $FeBr_2$ in 13 different DES systems,[54] in which the DES components serve a secondary role as the supporting ligand for the ATRP process. The RAFT polymerization of 2-hydroxyethylmethacrylate (HEMA) was performed by Santha Kumar and Singha[55] in reline and monitored by DSC, which showed greatly enhanced reaction kinetics and higher conversion compared to polymerization in the bulk, in DMF and in various ionic liquids. A similar phenomenon was observed by Li and Yu,[56] who performed the PET-RAFT polymerization of MMA, methyl acrylate, dimethylacrylamide and styrene in a tetrabutylammonium chloride/ethylene glycol DES; the rate of polymerization was significantly higher (4.5×) in the DES compared to in DMSO.

Monomers for ROP have also been used to prepare PE systems to enable the preparation of polyesters under relatively mild conditions. L-Lactide (LA) formed a 1 : 1 eutectic with trimethylene carbonate (TMC) which had a melting point of 23 °C;[57] this mixture was used to selectively form the homopolymer of LA at room temperature using benzyl alcohol as initiator and DBU as catalyst. By operating at temperatures above the glass transition of PLA, LA-TMC copolymers were successfully produced. Perez-Garcia and co-workers[58] prepared eutectics based on LA and CL in a 30 : 70 mass ratio (melting point −19 °C) to form polyester blends based on the selective polymerization of these two monomers within the continuous phase of a high internal phase emulsion (HIPE) to yield an open cell foam.

In this work, we report the formation and characterization of a PE based on NIPAM and CL, as a polymerizable mixture that is amenable to both (controlled) radical and ring-opening polymerization mechanisms. This is, to our knowledge, the first report of a binary PE where both components are polymerized *via* a different mechanism in the one system. *Via* a simple heating and stirring approach, NIPAM : CL PEs were formed that persist as stable, viscous liquids at room temperature that can polymerized under mild conditions. To demonstrate the behaviour of these PEs, we report the block copolymer synthesis of PNIPAM-*b*-PCL, achieved using a modified RAFT agent that serves both as CTA and ROP initiator. This polymerization was achieved at room temperature using the PET-RAFT process to polymerize NIPAM with blue light and a ruthenium photocatalyst, as well as the anionic ROP of CL mediated by an appropriate catalyst, with no deoxygenation. Under what are essentially solvent-free conditions, the polymerization proceeded at higher rates than equivalent reactions in organic solvents, with good molar mass control of the resulting polymers.

Experimental

Materials

N-Isopropylacrylamide (NIPAM; 97%) was purchased from Sigma-Aldrich. ε-Caprolactone (CL; 98%) was purchased from Combi-Blocks. Ethylene glycol (99%), *N*,*N*-dicyclohexylcarbodiimide (DCC, 99%), 4-(dimethylamino)pyridine (DMAP, ≥99%) and $[Ru(bpy)_3(PF_6)_2]$ (97%) were all purchased from Sigma-Aldrich and used as received. 2-(*n*-Butyltrithiocarbonate)-propionic acid (BTPA) was synthesized according to literature procedures.[59] Tin(II) 2-ethyl hexanoate (TEHA) was purchased from Aldrich. Liquid monomers were passed through a short column of basic alumina to remove inhibitors; all other reagents were used as received without any further purification.

Analysis

1D and 2D (ROESY and DOSY) proton (^{1}H) NMR spectra were acquired using a Bruker AVANCE III HD 400 MHz spectrometer equipped with a 5 mm broadband tuneable probe (BBFO) with a *z*-gradient. NMR spectra of PEs were obtained by placing the

sample in a 5 mm NMR tube; D_2O was placed in sealed capillary tube and inserted into the NMR tube for locking and shimming the sample and indirect referencing relative to the NMR standard sodium trimethylsilylpropanesulfonate (DSS). Spectra were recorded at 27 °C. 1D ^{1}H NMR spectroscopy was used to determine the fractional conversion of monomer to polymer by comparing the integral of vinylic protons of NIPAM ($\delta_H \sim 6.15$ ppm) and the ester group of ε-caprolactone ($\delta_H \sim 4.25$ ppm) before and after polymerization to an internal reference (DMF: $\delta_H = 3.30$ ppm). Deuterated chloroform ($CDCl_3$) was used as the NMR solvent for analysis of the copolymer.

Differential scanning calorimetry (DSC) experiments were performed using a PerkinElmer DSC 8000 instrument using an empty pan for reference. In a representative analysis, ~14 mg of freshly prepared PE was placed inside an aluminium pan. Nitrogen was used as carrier gas. The sample was heated from −45 to 60 °C at a rate of 5 °C min^{-1}, followed by an isothermal holding step at 60 °C for 5 min, and finally a cooling cycle from 60 to −45 °C at the same rate. Three loops of this sequence were performed. The DSC of prepared block copolymers was performed by heating the sample from −70 to 150 °C at a rate of 2 °C min^{-1}.

Thermogravimetric analysis (TGA) was carried out using a Setaram LABSYS Evo TG-DSC 1600C instrument. An aluminium oxide crucible (100 μL) was used to hold the sample in the furnace. The sample (~15 mg) was heated from 25 to 600 °C at a rate of 10 °C min^{-1} in a nitrogen atmosphere.

Polymer molar mass distributions were determined *via* using a Shimadzu system with refractive index detection (RID-10A), four Phenogel columns (10^5, 10^4, 10^3 and 500 Å pore size) and THF as eluent (flow rate 1 mL min^{-1}). All polymer samples were dissolved overnight in the eluent at a concentration ~3 mg mL^{-1}, then filtered through a 450 nm nylon filter. The columns were housed in a CTO-10AC VP Shimadzu column oven set at 40 °C. The system was calibrated with poly (methyl methacrylate) (PMMA) standards with molecular weights of 200 to 69 000 Da.

Dynamic light scattering (DLS) measurements were measured by using a Malvern ZetaSizer Nanoseries instrument integrated with DTS software. The measurement was carried out at 298 K using a 4 mW He–Ne laser with wavelength 633 nm. The scattering angle was 173°. Results were based on the average values of three independent measurements at intervals of 2 °C intervals within the temperature range of 20 to 40 °C.

Viscosity measurements were performed at 25 °C using an Atago Viscometer; the spindle speed was 200 rpm.

The light source for photopolymerization experiments was prepared from blue LED strips (λ = 472 nm, whole strips 10.4 V and 260 mA and each individual LED drops 2.9 V at ~10 mA) housed inside a circular stainless steel reactor, covered with aluminium foil. There were three LEDs in a group in series with a 130-Ohm resistor, and there were 28 groups in the strip.

Synthesis of non-ionic polymerizable eutectics. Non-ionic PEs were prepared from mixtures of NIPAM (*N*-isopropylacrylamide) and CL (ε-caprolactone) in various mole ratios. The two reagents were added to a sealed flask and placed under a nitrogen atmosphere, followed by heating at 50 °C for 1 h with continuous magnetic stirring. The resulting clear viscous liquid was allowed to cool slowly to visually determine the freezing onset temperature. These mixtures were also analyzed *via* DSC.

Synthesis of hydroxyl chain transfer agent (HCTA). HCTA was synthesized according to literature procedures.[26] Briefly, BTPA (0.50 g, 2 mmol), ethylene glycol (0.40 g, 6.4 mmol), DCC (0.43 g, 2.08 mmol) and DMAP (5 mg, 0.041 mmol) were dissolved in THF (10 mL) and magnetically-stirred at room temperature. After 12 h, the white precipitate was removed by filtration, the filtrate was concentrated under reduced pressure and the ensuing residue was subjected to flash column chromatography (silica gel, 20% EtOAc/hexanes v/v) to provide HCTA as a yellow oil (391 mg, 70% yield).

Synthesis of block copolymers from polymerizable eutectics by one pot PET-RAFT and ROP approach. A NIPAM–CL PE was prepared from 1 : 1 molar ratio mixtures of NIPAM (0.31 g, 2.7 mmol) and CL (0.31 g, 2.76 mmol) by heating at 50 °C for 0.5 h with continual magnetic stirring at 300 rpm. HCTA (13 mg, 0.046 mmol), a DMSO stock solution of [Ru(bpy)$_3$(PF$_6$)$_2$] (60 μL, 4.4×10^{-5} mmol) and tin(II) 2-ethylhexanoate (TEHA) (11 mg, 0.046 mmol) were added directly to the PE with continual stirring until all components were dissolved. The solution was then irradiated with blue light in a custom-built photoreactor. Samples were withdrawn periodically for GPC and NMR analysis. The polymerization was quenched by removal from light, the flask opened to the air and cooled on ice. The polymer was isolated by precipitation from THF to hexanes and dried under vacuum.

Results and discussion

Preparation and characterization of non-ionic polymerizable eutectics

NIPAM : CL polymerizable eutectics (PE) were prepared by mixing NIPAM and CL at various mole ratios and heating at 50 °C for 1 h. This process is depicted in Fig. 1A. NIPAM is solid at room temperature with melting point of 64 °C, while CL is a liquid at room temperature with melting point −1 °C. Upon heating these mixtures at 50 °C, clear viscous liquids formed that remained in the liquid state even upon cooling to room temperature.

Due to the low melting and freezing point onset of these mixtures, the thermal properties were studied *via* a combination of differential scanning calorimetry (DSC) and thermogravimetric analysis (TGA). An analysis of melting (when heated) and melt crystallization (when cooled) transitions across separate heating and cooling DSC loops showed that the 1 : 1 NIPAM : CL mixture displayed the lowest reproducible melt onset and melt crystallization temperatures (−8.4 ± 0.3 °C and −25.6 ± 0.5 °C, respectively; see Fig. 1B as well as Fig. S1, ESI†) TGA thermograms (Fig. S2, ESI†) showed that the NIPAM : CL 1 : 1 PE possessed equivalent thermal stability rela-

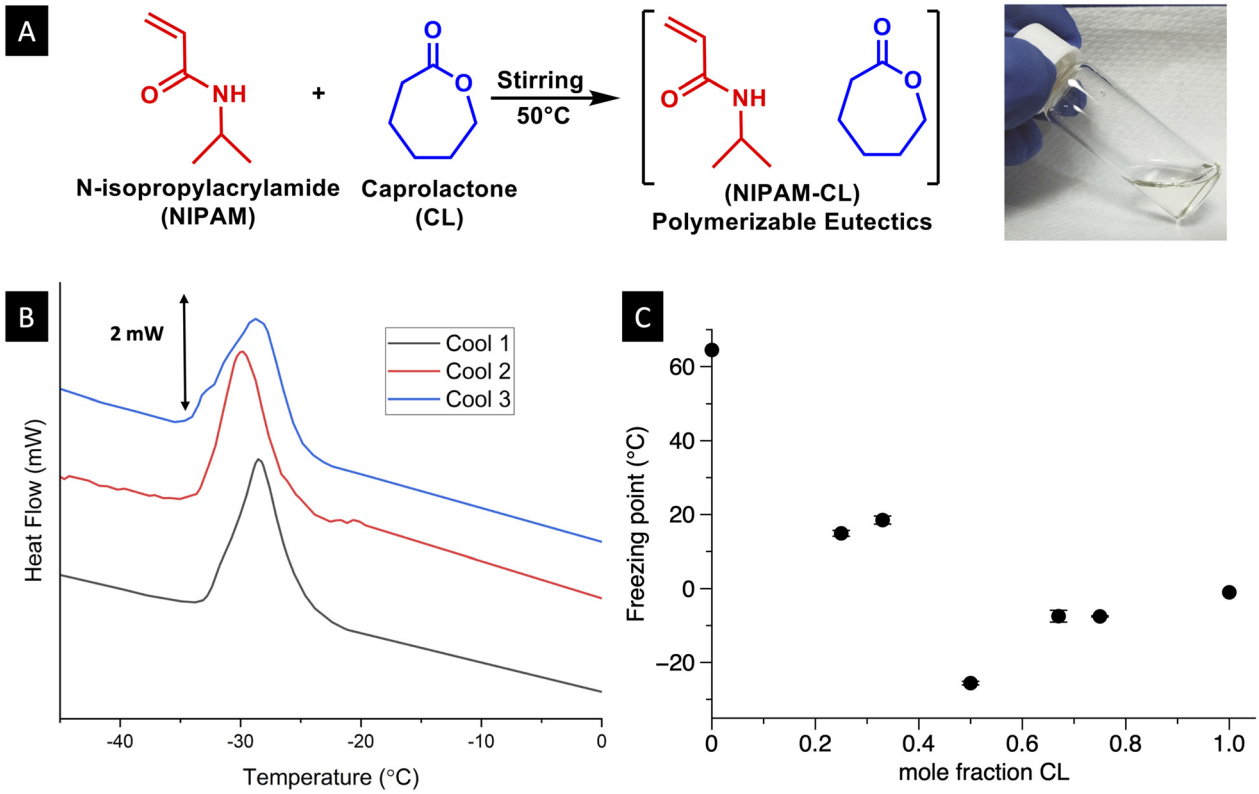

Fig. 1 (A) Schematic overview of the preparation of NIPAM–CL based polymerizable eutectics, with a digital photograph (right) showing the resulting liquid at room temperature; (B) DSC thermogram (cooling rate 2 °C min^{-1}) of the 1 : 1 NIPAM : CL PE (all three loops shown, data offset for clarity); (C) onset of freezing point for NIPAM : CL mixtures at various mole fractions of CL.

tive to the individual components of NIPAM and CL. A residual mass of ~20% was observed for the 1 : 1 PE, the origin of which is unclear. For the remainder of this work we primarily focused on the 1 : 1 PE. However, it should be noted that the versatility of this system allows for other mole ratios to serve as polymerizable systems.

To understand the hydrogen bonding network within the PE structure, a combination of 1D and 2D ^{1}H NMR spectroscopic experiments were performed consistent with our previous studies.[42,46] As expected, the spectrum of the eutectic in D_2O is identical to the spectrum of the mixed starting components (Fig. 2A–D). This is because the supramolecular structure is destroyed in this solvent and highlights that there were no side reactions occurring between NIPAM and CL during the eutectic formation. Spectrum E (Fig. 2E) was obtained by placing a D_2O-filled capillary in the neat PE sample. This demonstrated that the molecular species present in the PE are consistent with the parent components. The spectrum exhibits broad resonances due to the high viscosity of the eutectic, which was measured to be 10.6 cP at 298 K, as well as a systematic downfield shift of all resonances that likely derives from hydrogen bonding. Integration of all resonances in Spectrum E supported the proposed 1 : 1 composition of the PE (Fig. S3, ESI†). ^{1}H–^{1}H ROESY spectra (Fig. 3A) were consistent with the high level of association between NIPAM and CL. This is evident from the presence of off-diagonal cross-peaks that are sufficiently close to one another to enable spin–spin relaxation despite not being chemically bonded to one another.

The high viscosity of the PEs were reflected in the significant decrease of the self-diffusion coefficient D of the components, as determined by the results of the ^{1}H DOSY NMR experiment shown in Fig. 3B. In the ^{1}H NMR spectrum of the PE, the self-diffusion coefficients of NIPAM and CL were $\log_{10}(D/m^2\ s^{-1}) = -10.00 \pm 0.06$ and -9.80 ± 0.01, respectively. We have previously reported the self-diffusion coefficient of NIPAM in D_2O at this temperature to be $\log_{10}(D/m^2\ s^{-1}) = -9.1 \pm 0.03$,[42] indicating close to an order of magnitude reduction in the diffusion coefficient within the eutectic structure. The high viscosity of the reaction medium and low diffusion coefficient of the reacting species has implications for polymerization kinetics (see later discussion).

Photoinduced block copolymer synthesis by simultaneous PET-RAFT and ROP of PE. Herein we report the room temperature, solvent-free synthesis of a PNIPAM-*b*-PCL block copolymer using our NIPAM : CL PE system and a dual-functional initiator/chain transfer agent (HCTA). This was achieved by the simultaneous PET-RAFT polymerization of NIPAM using $[Ru(bpy)_3](PF_6)_2$ as a photocatalyst, in addition to the ring-opening polymerization (ROP) of CL catalysed by tin(II) 2-ethyl-

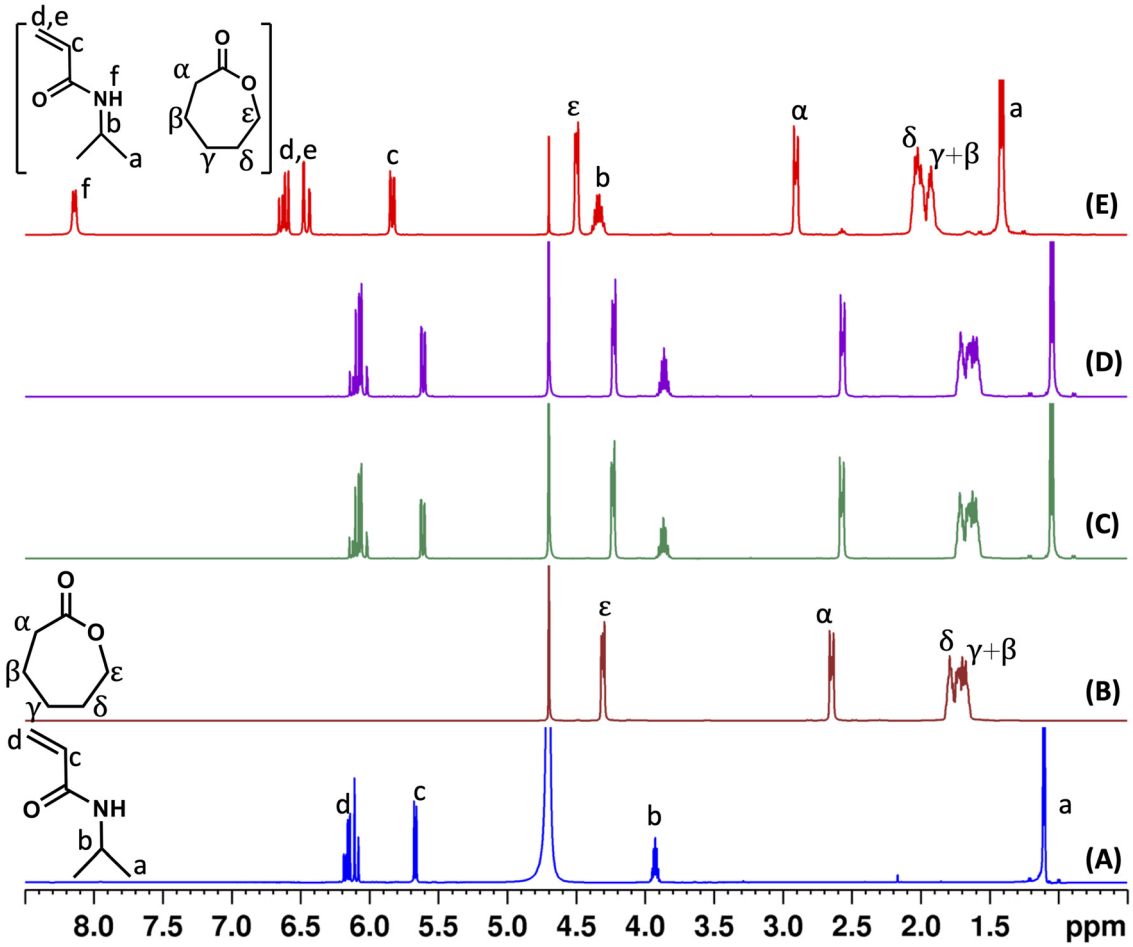

Fig. 2 ^{1}H NMR spectra of (A) NIPAM; (B) CL; (C) a 1 : 1 mixture of NIPAM and CL in D_2O; (D) 1 : 1 NIPAM : CL PE in excess D_2O; (E) 1 : 1 NIPAM : CL PE obtained with a D_2O-filled capillary placed in the sample.

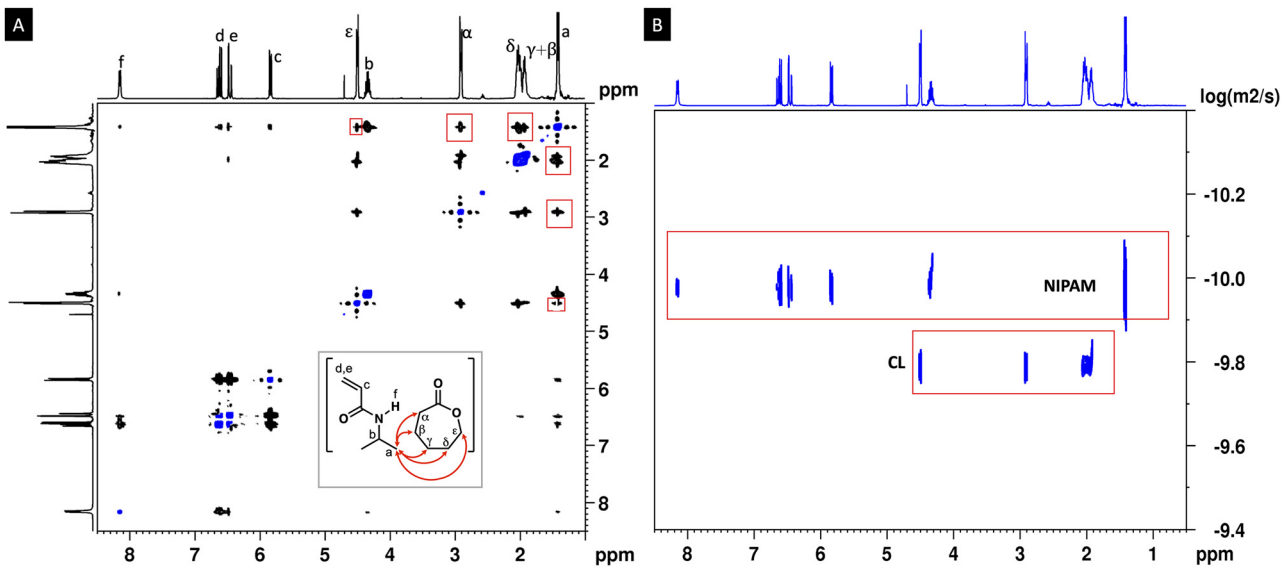

Fig. 3 (A) ^{1}H–^{1}H ROESY NMR spectrum of a 1 : 1 NIPAM : CL PE. (B) ^{1}H DOSY NMR spectrum of the 1 : 1 NIPAM : CL PE at 298 K.

hexanoate (TEHA) at ambient temperature. The HCTA possesses a terminal alcohol group (acting as the initiator for ROP) on the R-group of the RAFT agent, which itself facilitates the RDRP of NIPAM. During the polymerization, the PE serves both as the monomer(s) as well as the solvent for polymerization. The synthesis of PNIPAM-*b*-PCL is shown in Fig. 4A. For simultaneous PET-RAFT and ROP polymerization a reaction mixture with [NIPAM–CL] : [HCTA] : [TEHA] : $[Ru(bpy)_3](PF_6)_2$ = (60 : 60): 1 : 1 : 0.001 was employed.

^{1}H NMR spectroscopy was used to monitor the simultaneous PET-RAFT and ROP polymerization processes. Representative ^{1}H NMR spectra are presented in Fig. S4 (ESI†), which show the decrease in resonances at δ_H 4.25 ppm (assigned to the –OC$\underline{H}_2$ group within CL) and δ_H 5.50–6.30 ppm (assigned to the vinyl group within NIPAM). In addition, the appearance of resonances at δ_H 4.15 ppm (attributed to the –OC$\underline{H}_2$ group of PCL) and δ_H 1.11 ppm (attributed to the methyl groups of PNIPAM) are consistent with the successful PET-RAFT polymerization of NIPAM and ROP of CL from PE.

The reaction was sampled and analysed by ^{1}H NMR spectroscopy and GPC at various time intervals to determine both the fractional conversion of monomer to polymer and molecular weight determination. NMR spectroscopic analysis revealed a sharp increase in monomer conversion at early time periods (53% for NIPAM and 28% for CL after only 30 minutes), reaching a conversion of 88% and 48% for NIPAM and CL, respectively, after 6 h (Fig. 4B). The final conversions were comparable when the PE was degassed with nitrogen (78% and 44% respectively). The polymerization of both monomers was shown to follow pseudo-first order polymerization kinetics (see Fig. S9, ESI†). GPC analysis of the samples in THF indicated the formation of polymers of relatively low dispersity ($1.22 \leq Đ \leq 1.41$) and increasing number average molecular weight with increasing fractional conversion (Fig. 4C and D). The M_n value (by GPC) of the polymer after 6 h reaction time was 9053 Da, which was in relatively good agreement with the theoretical M_n based on the initial [monomers] : [RAFT] ratio and fractional conversion (9533 Da, see ESI†). Peak assignment of the ^{1}H NMR spectra of the isolated and purified polymer (Fig. S5, ESI†) supported the successful formation of PNIPAM-*b*-PCL, with relative peak integration indicating ~52 repeat units of NIPAM and ~28 repeat units of CL within the copolymer structure ($M_{n,NMR}$ = 9392 Da). TGA of the copolymer (Fig. S6, ESI†) showed a small mass loss at approximately 100–125 °C (attributed to the loss of moisture in the sample), followed by an initial gradual loss in the region ~150–350 °C due to the statistical chain cleavage of the polyester chains of PCL *via* ester pyrolysis;[60,61] rapid mass loss in the region ~410–450 °C is attributed to the degradation of the NIPAM units within the backbone. DSC analysis of the block copolymer (Fig. S8†) is further supportive of the block copolymer structure with observable melting point and glass transitions corresponding the PCL and PNIPAM blocks.

Further analysis of the polymer *via* FTIR spectroscopy and DLS was used to support the PNIPAM-*b*-PCL structure. The ATR-FTIR spectra (Fig. S7, ESI†) of the material showed a peak at 1715 cm^{-1}, assigned to C=O stretching in PCL, and PNIPAM characteristic peaks at 3306 cm^{-1} (N–H), 1644 cm^{-1} (amide C=O) and 1543 cm^{-1} (amide N–H) were also observed. Furthermore, absorption peaks at 1387 and 2874–2973 cm^{-1} are consistent with methylene groups present in the PCL backbone.[62] As a further demonstration of polymer structure, block copolymer nanoparticles were obtained by dissolving the material at a concentration of 5 mg mL^{-1} in THF (a good solvent for both PNIPAM and PCL), followed by a slow addition of water (in eight-fold excess by volume) over a period of twenty minutes followed by two days of dialysis against de-

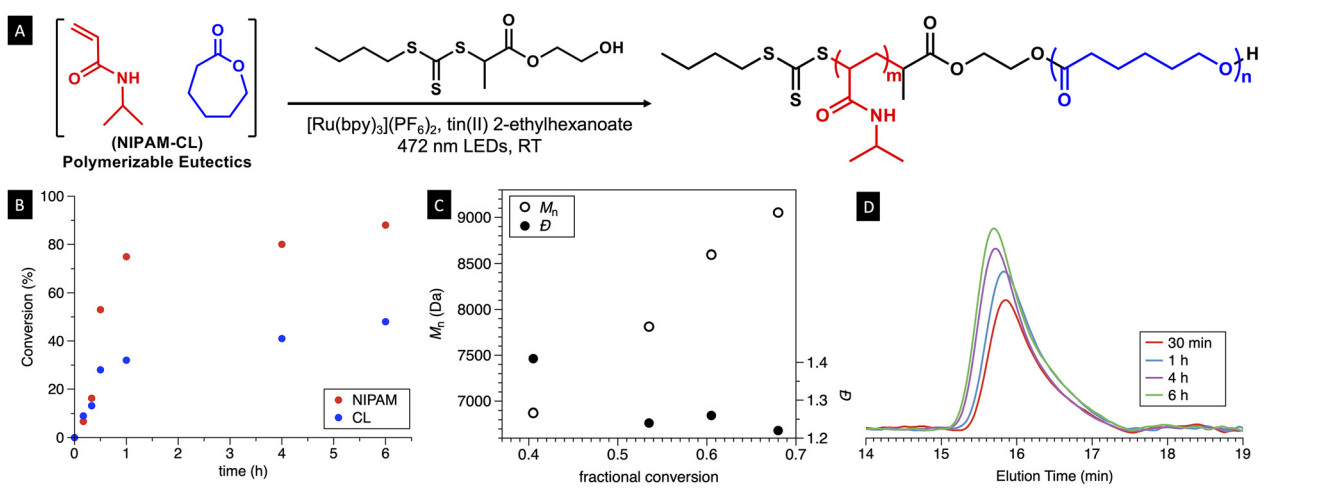

Fig. 4 (A) Schematic overview of block copolymer synthesis *via* the simultaneous PET-RAFT/ROP of a 1 : 1 NIPAM : CL PE using an alcohol-containing RAFT agent (HCTA); (B) conversion of NIPAM (red data points) and CL (blue data points) as a function of time *via* simultaneous PET-RAFT/ROP; (C) evolution of M_n (unfilled data points) and dispersity (filled data points) as a function of total monomer conversion as determined by GPC; (D) GPC chromatograms of PNIPAM-*b*-PCL copolymers as a function of reaction time (data scaled with respect to conversion for clarity).

ionized water to remove the THF.[63] DLS analysis of the dispersion (Fig. 5) revealed nanoparticles of hydrodynamic diameter 258 ± 24 nm (PDI = 0.47) at 20 °C. The dispersion is transparent at this temperature, and given the relative solubilities of the PNIPAM and PCL in water, we posit a nanoparticle structure with a PCL core and PNIPAM corona. Due to the thermoresponsive behaviour of PNIPAM,[64] a large increase in hydrodynamic diameter was observed (6933 ± 117 nm (PDI 0.27) at 40 °C) as the temperature increased beyond the lower critical solution temperature (LCST) of 32 °C and the dispersion became turbid (see Fig. 5 inset). This result is supportive of the PNIPAM-*b*-PCL structure given the collapse of PNIPAM chains at the particle surface at this increased temperature, similar to the work of Vandewalle *et al.*[25]

One of the major advantages of the polymerizable eutectic concept is that the need for other solvents is obviated. In addition, several groups (including ours) have observed large increases in polymerization rate in eutectics compared to the equivalent polymerizations in more common solvents.[40–42,47,65] To that end, we performed the equivalent PET-RAFT/ROP process of 1 : 1 mixtures of NIPAM and CL in a two different solvents suitable for the preparation of this block copolymer (THF and dioxane) at 50% w/w relative to monomer. Over the same reaction time, the fractional conversion of NIPAM and CL was considerably lower in both THF and dioxane compared to the PE (Fig. 6). A semi-logarithmic plot (Fig. S9, ESI†) shows that the pseudo-first order propagation rate coefficient k_p^{app} for the polymerization of NIPAM was greater in the PE system by a factor of ~5 (in dioxane) and 3.8 (in THF). Assuming a constant rate of radical generation, this relative rate increase is likely due to a combination of two main factors: (i) a decrease in the bimolecular termination rate coefficient between terminating radicals due to the high viscosity of the reaction medium, and (ii) an increase in the propagation rate coefficient, potentially due to complexation

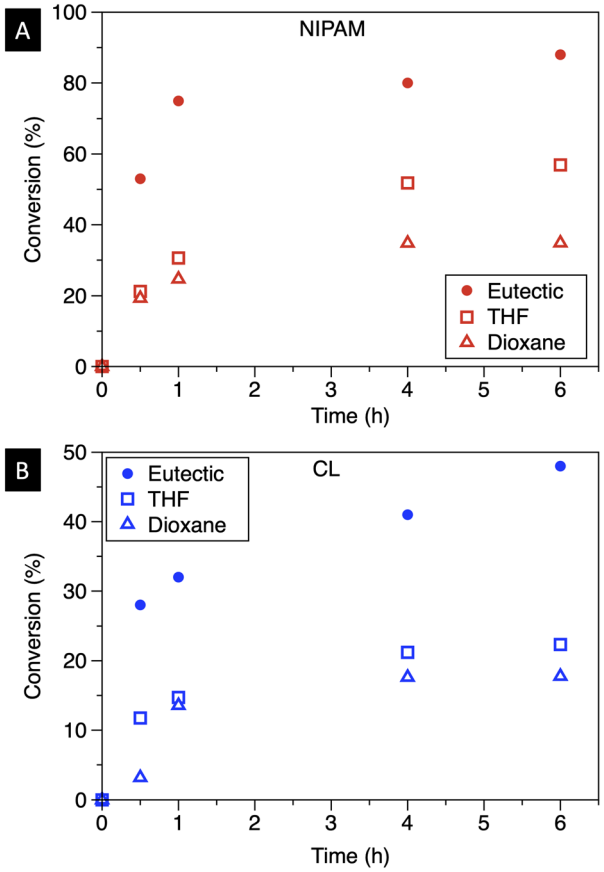

Fig. 6 Conversion of (A) NIPAM and (B) CL *versus* time in 1 : 1 PE, THF and 1,4-dioxane. For associated semi-logarithmic plots, see ESI.†

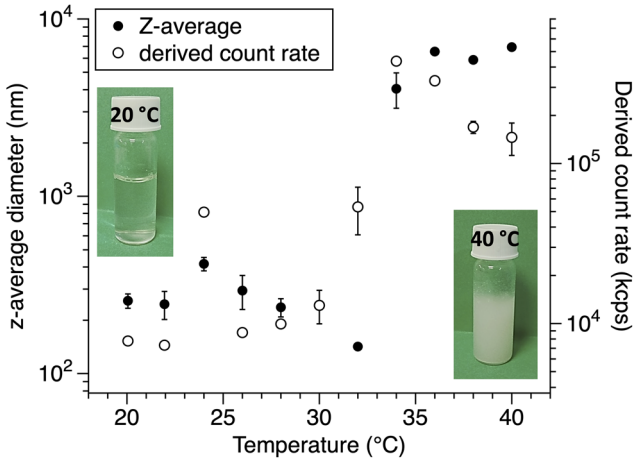

Fig. 5 *Z*-Average diameter (filled data points) and derived count rate (unfilled data points) as a function of temperature of PNIPAM-*b*-PCL in water, as determined by DLS. Inset are photographs of the sample at 20 °C (left) and 40 °C (right), respectively.

via hydrogen bonding; this has been seen previously for monomers that can hydrogen bond with the polymerization solvent.[66–68] An increase in the rate of polymerization of CL was also observed when the PE was used in comparison to both THF and dioxane; the rate enhancement was approximately 2.5 in both solvents. In combination, the overall polymerization rate for the synthesis of this block copolymer is significantly increased compared to solution polymerization, while also achieving high total conversion of monomer to polymer.

Given the distinct polymerization mechanisms and catalysts used for both NIPAM and CL polymerization, the potential orthogonality of each synthetic step is an appealing concept for control over the reaction process. To evaluate this, we performed the PET-RAFT polymerization of NIPAM in blue light for 3 h, in the absence of any TEHA to initiate CL. The polymerization was shown to be selective for NIPAM (42%), whereas the conversion of CL was zero. Upon addition of TEHA to the reaction mixture (while continuing irradiation with blue light), the conversion of CL was 37% after a further 3 h (with NIPAM increasing to 63%, see Fig. 7A).

In the reverse case, we performed the reaction in the dark, with all reagents (HCTA, $[Ru(bpy)_3](PF_6)_2$ and TEHA present. No reaction was observed for either monomer over a period of

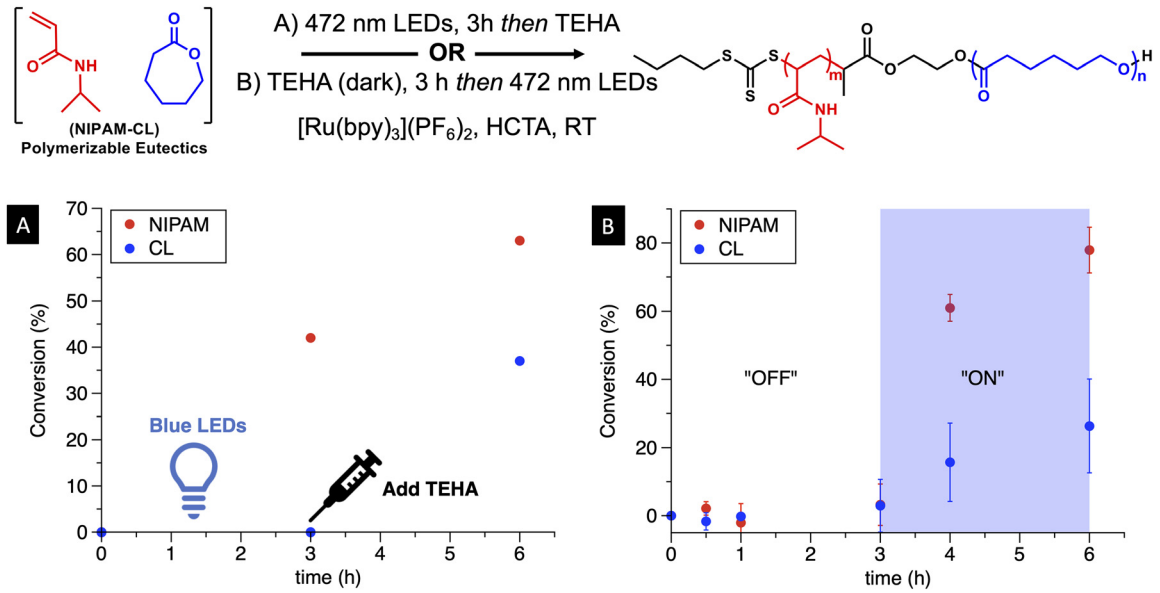

Fig. 7 Sequential polymerization of NIPAM : CL PE *via* PET-RAFT and ROP mechanisms to generate PNIPAM-*b*-PCL copolymers. (A) Blue light irradiation from t = 0 (in the absence of TEHA as ROP catalyst), followed by addition of TEHA after t = 3 h; (B) system kept in the dark for 3 h (TEHA present), followed by blue light irradiation after t = 3 h.

3 h. Upon blue light irradiation, both monomers were successfully polymerized (NIPAM = 77%, CL = 29%, see Fig. 7B). Thus, NIPAM was able to be successfully polymerized in an orthogonal fashion within our PE systems, whereas CL polymerization could only be achieved in the presence of blue light irradiation. The fundamental mechanistic basis of these observations remains unclear, however, we postulate that the TEHA may not effectively generate an alkoxide for the ROP of CL in the absence of blue light. Future work will focus on undertaking a dedicated, extensive study to better understand this nuance, as part of broader investigations that will look to develop a NIPAM and CL copolymerization that operates with complete orthogonality.

Conclusions

In this work, we report the first preparation and characterization of a binary polymerizable eutectic (PE) based on components that are amenable to two distinct mechanisms of polymerization. These PEs, which were viscous liquids at room temperature, were used as the precursor to prepare block copolymers *via* the simultaneous RAFT and ring-opening polymerization (ROP) of NIPAM and CL using a bifunctional initiator/chain transfer agent. This process was achieved at room temperature under relatively benign conditions, utilizing the PET-RAFT process to polymerize NIPAM in the presence of $[Ru(bpy)_3(PF_6)_2]$ and blue light, in addition to tin 2-ethylhexanoate (TEHA) to initiate the ROP process. Polymers of relatively low dispersity were formed that showed an increase in number average molar mass with conversion, as anticipated. The simultaneous polymerization of NIPAM and CL within the PE exhibited significantly enhanced polymerization kinetics compared to the equivalent polymerizations in common organic solvents, highlighting a major benefit of this approach compared to currently established techniques. Given the simplicity of preparing these polymerizable eutectics, a one-pot (one-step) block copolymer synthesis pathway is realised, albeit in the presence of appropriate catalysts for each polymerization mechanism. We envisage that they will represent a convenient method to prepare composite materials based on both radical and ring-opening polymerization in the absence of any added solvents.

Author contributions

YN – investigation, methodology, writing – original draft, writing – review and editing; MKS – investigation, methodology, validation, writing – original draft, writing – review and editing; ACB –methodology, supervision, writing – original draft, writing – review and editing; SCT – conceptualization, methodology, supervision, writing – original draft, writing – review and editing.

Conflicts of interest

There are no conflicts to declare.

Acknowledgements

YN acknowledges the University of Tasmania (UTAS) for the provision of a postgraduate scholarship. ACB's contributions

were supported by an ARC Future Fellowship (FT200100049). We thank the UTAS Central Science Laboratory for providing access to NMR spectroscopy services and Dr James Horne for assistance with NMR spectroscopy.

References

1 N. Corrigan, K. Jung, G. Moad, C. J. Hawker, K. Matyjaszewski and C. Boyer, *Prog. Polym. Sci.*, 2020, **111**, 101311–101326.
2 K. Matyjaszewski, *Macromolecules*, 2012, **45**, 4015–4039.
3 C. J. Hawker, A. W. Bosman and E. Harth, *Chem. Rev.*, 2001, **101**, 3661–3688.
4 N. P. Truong, G. R. Jones, K. G. E. Bradford, D. Konkolewicz and A. Anastasaki, *Nat. Rev. Chem.*, 2021, **5**, 859–869.
5 S. Perrier, *Macromolecules*, 2017, **50**, 7433–7447.
6 N. J. Treat, B. P. Fors, J. W. Kramer, M. Christianson, C.-Y. Chiu, J. Read de Alaniz and C. J. Hawker, *ACS Macro Lett.*, 2014, **3**, 580–584.
7 Y. Zhao, M. Yu, S. Zhang, Y. Liu and X. Fu, *Macromolecules*, 2014, **47**, 6238–6245.
8 B. P. Fors and C. J. Hawker, *Angew. Chem., Int. Ed.*, 2012, **51**, 8850–8853.
9 J. Xu, S. Shanmugam, H. T. Duong and C. Boyer, *Polym. Chem.*, 2015, **6**, 5615–5624.
10 J. Yeow, R. Chapman, A. J. Gormley and C. Boyer, *Chem. Soc. Rev.*, 2018, **47**, 4357–4387.
11 J. J. Li, X. Q. Pan, N. Li, J. Zhu and X. L. Zhu, *Polym. Chem.*, 2018, **9**, 2897–2904.
12 C. H. Hornung, C. Guerrero-Sanchez, M. Brasholz, S. Saubern, J. Chiefari, G. Moad, E. Rizzardo and S. H. Thang, *Org. Process Res. Dev.*, 2011, **15**, 593–601.
13 M. Chen, Y. Gu, A. Singh, M. Zhong, A. M. Jordan, S. Biswas, L. T. Korley, A. C. Balazs and J. A. Johnson, *ACS Cent. Sci.*, 2017, **3**, 124–134.
14 T. Öztürk, M. N. Atalar, M. Göktaş and B. Hazer, *J. Polym. Sci., Part A: Polym. Chem.*, 2013, **51**, 2651–2659.
15 M. D. Rowe, B. A. G. Hammer and S. G. Boyes, *Macromolecules*, 2008, **41**, 4147–4157.
16 J. C. Chen, M. Z. Liu, H. H. Gong, G. J. Cui, S. Y. Lu, C. M. Gao, F. Huang, T. T. Chen, X. Y. Zhang and Z. Liu, *Polym. Chem.*, 2013, **4**, 1815–1825.
17 Z. H. Sun, B. Choi, A. C. Feng, G. Moad and S. H. Thang, *Macromolecules*, 2019, **52**, 1746–1756.
18 C. Chang, H. Wei, C. Y. Quan, Y. Y. Li, J. Liu, Z. C. Wang, S. X. Cheng, X. Z. Zhang and R. X. Zhuo, *J. Polym. Sci., Part A: Polym. Chem.*, 2008, **46**, 3048–3057.
19 A. G. O. de Freitas, S. G. Trindade, P. I. R. Muraro, V. Schmidt, A. J. Satti, M. A. Villar, A. E. Ciolino and C. Giacomelli, *Macromol. Chem. Phys.*, 2013, **214**, 2336–2344.
20 D. Mecerreyes, G. Moineau, P. Dubois, R. Jerome, J. L. Hedrick, C. J. Hawker, E. E. Malmstrom and M. Trollsas, *Angew. Chem., Int. Ed.*, 1998, **37**, 1274–1276.
21 S. J. Shin, Y. C. Yu, J. D. Seo, S. J. Cho and J. H. Youk, *J. Polym. Sci., Part A: Polym. Chem.*, 2014, **52**, 1607–1613.
22 Y. Xia, G. M. Scheutz, C. P. Easterling, J. Zhao and B. S. Sumerlin, *Angew. Chem., Int. Ed.*, 2021, **60**, 18537–18541.
23 H. U. Kang, Y. C. Yu, S. J. Shin and J. H. Youk, *J. Polym. Sci., Part A: Polym. Chem.*, 2013, **51**, 774–779.
24 R. F. Storey and J. W. Sherman, *Macromolecules*, 2002, **35**, 1504–1512.
25 S. Vandewalle, M. Van De Walle, S. Chattopadhyay and F. E. Du Prez, *Eur. Polym. J.*, 2018, **98**, 468–474.
26 C. Fu, J. Xu, M. Kokotovic and C. Boyer, *ACS Macro Lett.*, 2016, **5**, 444–449.
27 J. Xu, K. Jung, A. Atme, S. Shanmugam and C. Boyer, *J. Am. Chem. Soc.*, 2014, **136**, 5508–5519.
28 C. Fu, J. Xu and C. Boyer, *Chem. Commun.*, 2016, **52**, 7126–7129.
29 J. Xu, K. Jung and C. Boyer, *Macromolecules*, 2014, **47**, 4217–4229.
30 N. J. W. Penfold, J. Yeow, C. Boyer and S. P. Armes, *ACS Macro Lett.*, 2019, **8**, 1029–1054.
31 Y. Dai, J. van Spronsen, G. J. Witkamp, R. Verpoorte and Y. H. Choi, *Anal. Chim. Acta*, 2013, **766**, 61–68.
32 C. Florindo, F. Lima, B. D. Ribeiro and I. M. Marrucho, *Curr. Opin. Green Sustain. Chem.*, 2019, **18**, 31–36.
33 Y. Liu, J. B. Friesen, J. B. McAlpine, D. C. Lankin, S. N. Chen and G. F. Pauli, *J. Nat. Prod.*, 2018, **81**, 679–690.
34 M. Francisco, A. van den Bruinhorst and M. C. Kroon, *Angew. Chem., Int. Ed.*, 2013, **52**, 3074–3085.
35 E. L. Smith, A. P. Abbott and K. S. Ryder, *Chem. Rev.*, 2014, **114**, 11060–11082.
36 A. P. Abbott, D. Boothby, G. Capper, D. L. Davies and R. K. Rasheed, *J. Am. Chem. Soc.*, 2004, **126**, 9142–9147.
37 A. P. Abbott, G. Capper, D. L. Davies, R. K. Rasheed and V. Tambyrajah, *Chem. Commun.*, 2003, 70–71, DOI: **10.1039/b210714g**.
38 A. Paiva, R. Craveiro, I. Aroso, M. Martins, R. L. Reis and A. R. C. Duarte, *ACS Sustainable Chem. Eng.*, 2014, **2**, 1063–1071.
39 J. D. Mota-Morales, R. J. Sanchez-Leija, A. Carranza, J. A. Pojman, F. del Monte and G. Luna-Barcenas, *Prog. Polym. Sci.*, 2018, **78**, 139–153.
40 J. D. Mota-Morales, M. C. Gutierrez, I. C. Sanchez, G. Luna-Barcenas and F. del Monte, *Chem. Commun.*, 2011, **47**, 5328–5330.
41 J. D. Mota-Morales, M. C. Gutierrez, M. L. Ferrer, I. C. Sanchez, E. A. Elizalde-Pena, J. A. Pojman, F. Del Monte and G. Luna-Barcenas, *J. Polym. Sci., Part A: Polym. Chem.*, 2013, **51**, 1767–1773.
42 Y. Nahar, J. Horne, V. Truong, A. C. Bissember and S. C. Thickett, *Polym. Chem.*, 2021, **12**, 254–264.
43 A. Carranza, J. A. Pojman and J. D. Mota-Morales, *RSC Adv.*, 2014, **4**, 41584–41587.
44 A. Carranza, M. G. Perez-Garcia, K. Song, G. M. Jeha, Z. Diao, R. Jin, N. Bogdanchikova, A. F. Soltero,

M. Terrones, Q. Wu, J. A. Pojman and J. D. Mota-Morales, *ACS Appl. Mater. Interfaces*, 2016, **8**, 31295–31303.
45 M. G. Pérez-García, A. Carranza, J. E. Puig, J. A. Pojman, F. del Monte, G. Luna-Bárcenas and J. D. Mota-Morales, *RSC Adv.*, 2015, **5**, 23255–23260.
46 Y. Nahar, P. R. Wei, C. Cipriani, A. Khodabandeh, A. C. Bissember, E. B. Pentzer and S. C. Thickett, *ACS Appl. Polym. Mater.*, 2022, **4**, 8429–8440.
47 K. F. Fazende, M. Phachansitthi, J. D. Mota-Morales and J. A. Pojman, *J. Polym. Sci., Part A: Polym. Chem.*, 2017, **55**, 4046–4050.
48 K. F. Fazende, D. P. Gary, J. D. Mota-Morales and J. A. Pojman, *Macromol. Chem. Phys.*, 2020, **221**, 1900511–1900515.
49 R. Li, T. Fan, G. Chen, H. Xie, B. Su and M. He, *Chem. Eng. J.*, 2020, **393**, 124685–124692.
50 R. Li, G. X. Chen, M. H. He, J. F. Tian and B. Su, *J. Mater. Chem. C*, 2017, **5**, 8475–8481.
51 Y. Nahar and S. C. Thickett, *Polymers*, 2021, **13**, 447–469.
52 P. V. Mendonça, M. S. Lima, T. Guliashvili, A. C. Serra and J. F. J. Coelho, *Polymer*, 2017, **132**, 114–121.
53 L. Quirós-Montes, G. A. Carriedo, J. García-Álvarez and A. Presa Soto, *Green Chem.*, 2019, **21**, 5865–5875.
54 J. R. Wang, J. Y. Han, M. Y. Khan, D. He, H. Y. Peng, D. Y. Chen, X. L. Xie and Z. G. Xue, *Polym. Chem.*, 2017, **8**, 1616–1627.
55 A. R. S. Santha Kumar and N. K. Singha, *J. Polym. Sci., Part A: Polym. Chem.*, 2019, **57**, 2281–2286.
56 C.-Y. Li and S.-S. Yu, *Macromolecules*, 2021, **54**, 9825–9836.
57 O. Coulembier, V. Lemaur, T. Josse, A. Minoia, J. Cornil and P. Dubois, *Chem. Sci.*, 2012, **3**, 723–726.
58 M. G. Perez-Garcia, M. C. Gutierrez, J. D. Mota-Morales, G. Luna-Barcenas and F. Del Monte, *ACS Appl. Mater. Interfaces*, 2016, **8**, 16939–16949.
59 R. J. H. Christopher, J. Ferguson, D. Nguyen, B. T. T. Pham, R. G. Gilbert, A. K. Serelis, C. H. Such and B. S. Hawkett, *Macromolecules*, 2005, **38**, 2191–2204.
60 A. K. Mishra, N. K. Vishwakarma, V. K. Patel, C. S. Biswas, T. K. Paira, T. K. Mandal, P. Maiti and B. Ray, *Colloid Polym. Sci.*, 2014, **292**, 1405–1418.
61 M. L. A. Olivier Persenaire, P. Degée and P. Dubois, *Biomacromolecules*, 2001, **2**, 288–294.
62 Z. Duan, L. Zhang, H. Wang, B. Han, B. Liu and I. Kim, *React. Funct. Polym.*, 2014, **82**, 47–51.
63 J. Chen, M. Liu, H. Gong, Y. Huang and C. Chen, *J. Phys. Chem. B*, 2011, **115**, 14947–14955.
64 B. R. Saunders, *Langmuir*, 2004, **20**, 3925–3932.
65 S. Bednarz, M. Fluder, M. Galica, D. Bogdal and I. Maciejaszek, *J. Appl. Polym. Sci.*, 2014, **131**, 40608–40615.
66 M. L. Coote, T. P. Davis, B. Klumperman and M. J. Monteiro, *J. Macromol. Sci., Rev. Macromol. Chem. Phys.*, 1998, **C38**, 567–593.
67 G. Schmidt-Naake, I. Woecht, A. Schmalfuß and T. Glück, *Macromol. Symp.*, 2009, **275–276**, 204–218.
68 B. De Sterck, R. Vaneerdeweg, F. Du Prez, M. Waroquier and V. Van Speybroeck, *Macromolecules*, 2009, **43**, 827–836.